Study of intrinsic point defects in oxides of the perovskite family: I. Theory



1996 J. Phys.: Condens. Matter 8 6705

(http://iopscience.iop.org/0953-8984/8/36/021)

J. Phys.: Condens. Matter **8** (1996) 6705–6717. Printed in the UK

# Study of intrinsic point defects in oxides of the perovskite family: I. Theory

S A Prosandeyev, A V Fisenko, A I Riabchinski, I A Osipenko, I P Raevski and N Safontseva

Department of Physics, Rostov State University, 5 Zorge Street, 344090, Rostov on Don, Russia

Received 16 January 1996, in final form 10 May 1996

**Abstract.** Special features of atomic vacancies in oxides of the perovskite family have been studied within the framework of the Green function method. It has been shown that, in accordance with experiments, the oxygen vacancy has both shallow and comparatively deep levels corresponding to different charge states. The single-charged oxygen vacancy has a deep level and, hence, it could be a good trap for electrons. We shall show that, owing to interaction with the lattice polarization, an electron is captured by one of the neighbours to the vacancy ions. As a result the single-charged oxygen vacancy proves to be a dipole centre. Peculiarities in the optical absorption spectra connected with the single-charged oxygen vacancy are discussed.

## 1. Introduction

The thermal treatment of oxides of the perovskite family (OPFs) is known to lead to drastic change in electroconductivity. This is usually associated with the oxygen vacancies $V_O$. The vacancies are believed to arise on heating under vacuum, and to disappear under an oxidizing ambient. When $V_O$ arises, two electrons are released. This leads to an increase in the carrier concentration in conduction bands. The electrons, being bounded, can contribute also to the optical characteristics of the crystal. In particular, they can take part in optical absorption and emission processes.

The electronic structure of $V_O$ was studied within different cluster approaches [1–4] as well as in the framework of the Green function method [5–11]. All these studies were performed on the assumption that the symmetry of $V_O$ coincides with the point symmetry of the oxygen site in the ideal crystal. However, recently, it was shown that the single-charged $V_O^+$ may be a dipole centre [12–15]. In this case, an electron captured by $V_O$ predominantly localizes on one of the neighbours to the $V_O$ ions. So, in particular, by convention, such a centre in $SrTiO_3$ may be indicated as $Ti^{3+}V_OTi^{4+}$ (or, equally, as $Ti^{4+}V_OTi^{3+}$). For $KTaO_3$, it can be represented as $Ta^{4+}V_OTa^{5+}$ and, in the general case, as $M^{n-1}V_OM^n$ (figure 1).

In the present work, we shall study the electronic structure of the dipole defect of $M^{n-1}V_OM^n$ type. Now, we wish to emphasize that our theory is of a semiempirical nature. The values of some parameters of the theory were taken from the band-structure calculations (hopping integrals) and from experiment (atomic polarizabilities). Nevertheless, the qualitative results obtained seem to us to be of a general nature. In particular, the possibility of the existence of the dipole state of the oxygen vacancy in perovskites will be considered very carefully by taking into account both the covalent effect and the difference between the local and average fields. On the basis of the results obtained, optical absorption

0953-8984/96/366705+13$19.50  

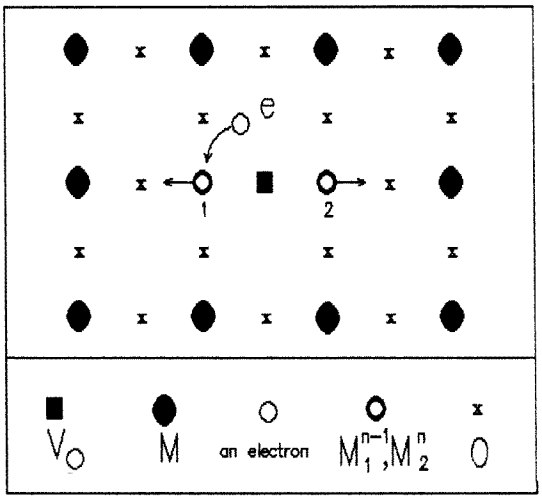


**Figure 1.** The geometry of $V_O^+$ in OPFs of the $AMO_3$ kind.

spectra will be computed. We have also carried out a calculation of the electronic structure of $V_K$ in $KTaO_3$. Experiments on optical absorption and emission spectra, electrical conductivity and photoconductivity will be discussed in part II of this paper.

## 2. The electronic structure of the oxygen vacancy

It was shown in [5–11] that it is convenient to apply the Green function method to the calculation of the electronic structure of point defects in OPFs. In this approach, the complex problem of solving the Schrödinger equation for the whole crystal containing a point defect is reduced to the comparatively simple problem of describing the scattering of the Bloch waves by the defect. In the Green function method the main characteristics of the defect can be exactly obtained by taking into account only the region where the potential is perturbed. Hereafter we shall use the term 'the potential' to mean the matrix of the potential in the atomic basis, while the 'perturbation potential' denotes the difference between the potentials in the perturbed and ideal crystals.

OPFs usually have a high static dielectric constant. In particular, $BaTiO_3$, $KNbO_3$, $PbTiO_3$ and others are known by their ferroelectric properties; $SrTiO_3$ and $KTaO_3$ are incipient ferroelectrics. In this connection, the perturbation potential produced by a point defect is of small radius. This markedly alleviates the problem and emphasizes proficiency in the use of the Green function method in this case.

Another special feature of OPFs is that they have an intermediate type of chemical bond. It is known that, in these crystals, dispersion in the electronic bands is caused by the nearest-neighbour interactions, i.e. by the interaction between the states of the M and O atoms [16]. Owing to this simplification, the electron energy as well as the density of the electron states can be described by analytical expressions (the Wolfram–Ellialtioglu [17] model). This circumstance helps us to construct convenient analytical formulae for calculating the ideal crystal Green functions [5–11]. In the present work, we shall employ just this approach. Note that the second-neighbour interactions were taken into account in [18] within the continued-fraction method. The results obtained were similar to those found by the Wolfram–Ellialtioglu model.

In the Green function method, the electron density of states can be expressed through

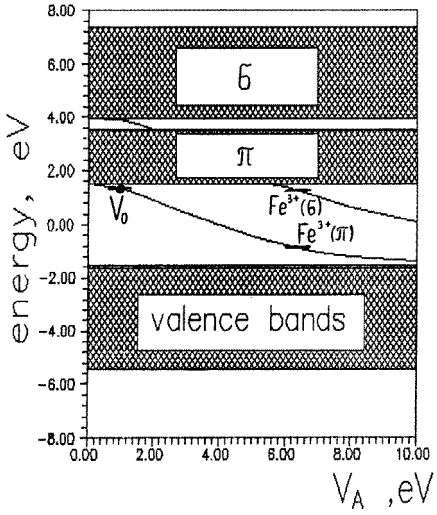


**Figure 2.** The dependence of the local state energies on the perturbation potential on a Ti site nearest to the oxygen vacancy in $SrTiO_3$. The positions of the $\pi$ and $\sigma$ $Fe^{3+}$ levels are also shown (the $Fe^{3+}$ ion substitutes for the $Ti^{4+}$ ion).

the diagonal element of the Green function:

$$N_L = -\frac{1}{\pi}\,\mathrm{Im}\,G_{LL} \tag{1}$$

where $\hat{G}$ is defined by the following equation:

$$\hat{G} = \hat{g} + \hat{g}\hat{V}\hat{G}. \tag{2}$$

Here $\hat{g}$ is the ideal-crystal Green function and $\hat{V}$ is the perturbation potential.

The local states can be found in the forbidden gap by solving the equation

$$\det \|\hat{I} - \hat{g}\hat{V}\| = 0. \tag{3}$$

Since in OPFs the potential $\hat{V}$ is of small radius, the matrix in (3) is of low dimensionality. Thus, this approach to seeking local states has no great quantitative difficulties.

The removal of the oxygen ion from a lattice site leads to a decrease in the number of atomic orbitals in the atomic basis of the tight-binding method. To take the orbitals of the oxygen ion away from the basis, one can employ the following procedure [19]. Let us assume that the oxygen ion orbitals are incorporated in an additional potential. Letting this potential go to infinity, we remove these orbitals from the basis. The same result could be achieved by causing the hopping integrals between the oxygen ion and its nearest neighbours to vanish.

In semiconductors of Si type, the removal of atom orbitals from the basis, i.e. the rupture of chemical bonds, leads to the appearance of a deep level in the forbidden gap [19]. In ionic crystals such as KCl, the cavity of the anion vacancy itself can capture an electron, forming an F centre [20]. In crystals with the intermediate type of chemical bond, the reason for the appearance of the local level in the forbidden gap can differ from both these cases. We are considering the possibility that the local state of $M^{n-1}V_OM^n$ type, where $n$ is the valence state of the ion M in the ideal crystal, occurs.

Figure 2 shows the result of the calculation of the local state energies in the forbidden gap of $SrTiO_3$ as a function of the perturbation potential on a Ti ion nearest to $V_O$. It is

seen that increasing the potential leads to splitting the level from the $\pi$ band and then from the $\sigma$ band. These local states preferentially localize on the ion Ti and oxygen ions nearest to it.

An estimation of the perturbation potential may be carried out in the continuous approach using the formula [6]

$$V_{vac}(r) = \begin{cases} -\dfrac{z}{\epsilon_0 r} & r > r_0 \\ -\dfrac{z}{\epsilon_\infty}\left(\dfrac{1}{r} - \dfrac{1}{r_0}\right) - \dfrac{z}{\epsilon_0 r} & r < r_0 \end{cases} \tag{4}$$

where $z$ is the effective charge of $V_O$, $r_0$ is the radius of the defect, and $\epsilon_\infty$ and $\epsilon_0$ are the high-frequency and static dielectric constants, respectively. Since, in OPFs, $\epsilon_0$ has very large values (e.g. $\epsilon_0 = 204$ for $KTaO_3$ at room temperature), equation (4) may be rewritten in the form

$$V_{vac}(r) = \begin{cases} 0 & r > r_0 \\ -\dfrac{z}{\epsilon_\infty}\left(\dfrac{1}{r} - \dfrac{1}{r_0}\right) & r < r_0 \end{cases}. \tag{5}$$

It was shown in [14] that the energy of polarization produced by $V_O^+$ decreases when the electron of $V_O^+$ is localized at one of two transition-metal ions nearest to the vacancy. Thus, an additional term is to be taken into account when calculating the perturbation potential

$$V_O = V_{vac} + V_{pol}. \tag{6}$$

This term, $V_{pol}$, is of polaronic nature and is simply a difference between the potentials in the symmetrical and asymmetrical states of the vacancy. The perturbation potential (6) is of negative sign and, thus, as can be seen from figure 2, it results in the appearance of a local state in the forbidden gap.

When an electron occupies the level, the electronic charge of the ion M increases. This increase, in turn, leads to a change in the perturbation potential. In the linear approximation we have

$$V_M = V_O + U\,\Delta q_M \tag{7}$$

where $U$ is the Hubbard parameter and $\Delta q_M$ is the change in the electron charge on the ion M caused by perturbation of the potential. In the Green function method, this charge may be found using the expression

$$\Delta q_M = -\frac{1}{\pi}\,\mathrm{Im}\left(\int^{\epsilon_F} (G_{MM} - g_{MM})\,\mathrm{d}\epsilon\right). \tag{8}$$

The parameter $U$ in (7) represents the energy of the interaction between two electrons located at the same centre. Its value may deduced from atomic structure calculations as a second derivative of the atomic energy on the occupation number or by interpolating experiments. We employed the value $U = 10$ eV [10].

The dependence of the perturbation potential on the occupation number leads to a dependence of the local state energy on the charge state of the vacancy. In other words, it implies that, generally speaking, the ionization potential of the electron captured by the vacancy does not coincide with the one-electron energy of the level in the forbidden gap and, furthermore, the ionization potential of the single-charged vacancy does not coincide with the ionization potential of the neutral vacancy.

The ionization potential may be obtained from the relation [21]

$$I = E(m-1) - E(m) = \int_{m}^{m-1} \epsilon(n)\,\mathrm{d}n \tag{9}$$

where $E(m)$ is the total energy of the point defect with $m$ electrons on the local level. It is interesting that, under reasonable assumptions, the integral in equation (9) may be found analytically [10]:

$$I = -\epsilon(m) - \frac{1}{2\epsilon_\infty} U f_M^4 \tag{10}$$

where $f_M$ is the projection of the wavefunction of the local state onto the basic state located on a metal ion nearest to the vacancy. The weight $f_M$ may be found from the linear equation

$$(\hat{1} - \hat{g}\hat{V})f = 0 \tag{11}$$

and the orthonormalization condition written in the form

$$-f\hat{V}\hat{g}'(\epsilon)\hat{V}f = 1. \tag{12}$$

Here $\hat{g}'(\epsilon)$ is the derivative of the Green function $\hat{g}(\epsilon)$ with respect to $\epsilon$.

The results of our calculations have shown that the ionization potential of the neutral vacancy is very small (it is several hundredths of an electronvolt), at any of the reasonable values of the model parameters. The corresponding one-electron wavefunction is spread over a wide region of the crystal near $V_O$. The single-charged vacancy has a deeper level (table 1). Its energy is several tenths of an electronvolt.

**Table 1.** The one-electron energies and ionization potentials of the single-charged oxygen vacancy in different crystals of the perovskite family ($z = 2|e|$).

| | $\epsilon(0)$ (eV) | $\epsilon(1)$ (eV) | $I$ (eV) |
|---|---|---|---|
| $CaTiO_3$ | 0.42 | 0.14 | 0.25 |
| $SrTiO_3$ | 0.46 | 0.14 | 0.26 |
| $BaTiO_3$ | 0.55 | 0.15 | 0.31 |
| $CaZrO_3$ | 0.41 | 0.12 | 0.23 |
| $SrZrO_3$ | 0.50 | 0.13 | 0.27 |
| $BaZrO_3$ | 0.51 | 0.12 | 0.27 |
| $BaHfO_3$ | 0.51 | 0.12 | 0.26 |
| $NaNbO_3$ | 0.30 | 0.11 | 0.18 |
| $KNbO_3$ | 0.38 | 0.12 | 0.22 |
| $NaTaO_3$ | 0.23 | 0.09 | 0.14 |
| $KTaO_3$ | 0.29 | 0.10 | 0.17 |

In the next section we shall show that, owing to the polaronic effect, the electron of $V_O^+$ is preferentially located at one of the ions M nearest to the vacancy. However, the direction of the dipole moment may be easily changed by quantum or thermal fluctuations and, in particular, by an applied electric or mechanical field.

## 3. Symmetry breaking at the oxygen vacancy in oxides of the perovskite family

First, symmetry breaking at the oxygen vacancy was proposed in [12, 13] on the basis of a theoretical analysis. It was proved there that the Hubbard interaction between electrons on transition-metal ions could cause symmetry breaking.

The first experimental evidence of this phenomenon was reached by the second-harmonic generation method in [22]. It was shown that nominally pure reduced samples of $KTaO_3$ have about $10^{18}$ $cm^{-3}$ dipole centres. The concentration of these centres was found to increase with further reduction in the samples and to decrease on oxidation.

The first theoretical computation of the geometry of $V_O$ in $SrTiO_3$ and $KTaO_3$ taking into account the lattice polarization was carried out in [14]. For this purpose, a small ($2 \times 3$ unit cells) cluster was used. It was found that the interaction of the electron captured by the vacancy with the lattice polarization results in symmetry breaking. The energy of the state where the electron was trapped at one of the metal ions nearest to the vacancy was proved to be lower than the energy of the state where the electron charge was uniformly distributed over the ions nearest to the vacancy.

In the present paper, we perform a much more careful investigation of the problem. The covalent bond effect will be taken into account. By using the Green function method, we shall evaluate the covalent energy gain and compare it with the polarization energy decrease. We shall show that the total energy consisting of these two parts decreases when the point symmetry of $V_O$ is broken. Furthermore, we use a correct asymptotic value of the electric field produced by the vacancy [23].

As in the Mott–Littletone model, we divide the crystal into two parts. The first includes 160 atoms which are treated by the most correct procedure. The second region comprises about 2000 atoms. The electric field on these atoms is believed to coincide with the correct asymptotic value obtained in [23].

If the Ta–O chemical bond were of pure ionic character the ionic charge of the oxygen contribution would equal $2e$. However, there is a strong covalent contribution to the Ta–O bonding. The results of band-structure calculations [16, 17] have shown that the charges of the Ta and O ions are $2.5e$ and $-1.2e$, respectively. These data correspond to the case when, because of covalent bonding, each Ta ion takes $-0.4e$ from each nearest O ion if one starts from the pure ionic charges: $5e$ for the Ta ion and $-2e$ for the O ion. The potassium atom is simply regarded as a donor for the $TaO_3$ sublattice. Hence, the K charge is $1e$.

When $V_O^{2+}$ is created (figure 1), two Ta–O bonds prove to be broken. This means that each of the two Ta ions acquires the additional charge $0.4e$. However, if the local state in the forbidden gap is occupied by an electron, we should add the charge of this electron. Our calculations have shown that approximately half the electron charge is localized on the two Ta ions and the remaining half is on the nearest ten oxygen ions. Thus, the additional charge of each Ta ion is $-0.25e + 0.4e = 0.15e$. This holds only for the symmetrical case. If symmetry breaking occurs, then the additional charge of one of the two Ta ions becomes $-0.5e + 0.4e = -0.1e$ and the additional charge of each of the five nearest oxygen ions is $-0.1e$. The additional charge of the other Ta ion is $0.4e$ while the additional charges of the five oxygen ions nearest to it vanish. Having performed the calculation of the polarization energy we have obtained that the asymmetrical state has a polarization energy 1.6 eV lower than the energy in the symmetrical case. This value is of the same order as that found in [14] for $SrTiO_3$ (unfortunately, the value found in [14] for $KTaO_3$ was incorrect because of a technical mistake).

A few words should be said about the quantitative influence of the choice of the additional atomic charges on the result. First of all, we should say that the energy of polarization quadratically depends on the total additional charge. Thus, the increase in the total additional charge will cause a quadratic increase in $V_{pol}$. Moreover, if one neglects the Ta–O covalent bonding and, as a consequence, the electron charge is localized on two Ta ions nearest the vacancy, then the polarization energy as well as $V_{pol}$ increase very strongly. Therefore, in the cases mentioned above, one can expect a sharp gain in the

polarization energy.

Now, let us discuss factors which stabilize the symmetrical state. As we have just seen, the covalent bond is one of these factors. It leads to a decrease in the additional charge connected with the captured electron. However, this is not the only way in which covalency influences the result. Owing to the covalent bond, there is an indirect interaction between two Ta sites and this interaction obviously stabilizes the symmetrical state. Thus, there is a necessity to evaluate the energy of the indirect interaction. The following is devoted to this point.

The contribution of the local electron state to the covalent energy can be evaluated from the expression

$$E_{cov} = \frac{1}{2}\sum_{ni}\sum_{mj} f_{ni} t_{ni,mj} f_{mj} \tag{13}$$

where $f_{ni}$ is the amplitude of the one-electron wavefunction of the local state on the $i$th atom of the $n$th unit cell and $t_{ni,mj}$ is the hopping integral for nearest neighbours. The amplitude $f_{ni}$ satisfies the following equation:

$$f_{ni} = \sum_{mj} g_{ni,mj}(\epsilon) V_{mj} f_{mj} \tag{14}$$

where $V_{mj}$ is the perturbation potential, $g_{ni,mj}$ is the Green function of the ideal crystal and $\epsilon$ is one of the roots of equation (3).

Inserting (14) into (13), we have

$$E_{cov} = \frac{1}{2}\sum_{ni}\sum_{mj} E_{cov}^{ni,mj} \tag{15}$$

where

$$E_{cov}^{ni,mj} = f_{ni} V_{ni} \sum_{ps}\sum_{uw} g_{ni,ps}(\epsilon) t_{ps,uw} g_{uw,mj}(\epsilon) V_{mj} f_{mj}. \tag{16}$$

The non-diagonal elements $E_{cov}^{ni,mj}$ are the interaction energies between the sites. Thus, only this quantity needs to be evaluated. To perform the summations in (16) over the lattice sites we shall employ the following manoeuvre. Let us write the equation defining the ideal-crystal Green function $\hat{g}$:

$$\sum_{mj}[(\epsilon - \epsilon_j)\delta_{nm}\delta_{ij} - t_{ni,mj}]g_{mj,ps} = \delta_{pn}\delta_{si}. \tag{17}$$

Here $\epsilon_j$ is the energy of the $j$th orbital in the cell. It is possible to express the matrix product $\hat{t}\hat{g}$ from (17) and to insert the result into equation (16). Hence, (16) is reduced to the form

$$-E_{cov}^{ni,mj} = f_{ni}^* V_{ni} g_{ni,mj}(\epsilon) V_{mj} f_{mj} - f_{ni}^* V_{ni} \sum_{ps}(\epsilon - \epsilon_s) g_{ni,ps}(\epsilon) g_{ps,mj}(\epsilon) V_{mj} f_{mj}. \tag{18}$$

The remaining sum may be treated as follows. Let us write the definition of the Green function through the eigenvalues and eigenstates of the electron Hamiltonian:

$$g_{ni,ps}(\epsilon) = \sum_{\tau \boldsymbol{k}} \frac{\langle i|\tau \boldsymbol{k}\rangle\langle \tau \boldsymbol{k}|s\rangle}{\epsilon - \epsilon_{\boldsymbol{k}}^{\tau}} \exp[-\mathrm{i}\boldsymbol{k}\cdot(\boldsymbol{R}^n - \boldsymbol{R}^p)] \tag{19}$$

where $\tau$ is the number of the electronic band. By using this expression, the summation over $p$ can be performed analytically. Indeed,

$$\sum_{p} \exp[\mathrm{i}\boldsymbol{R}^p \cdot (\boldsymbol{k} - \boldsymbol{q})] = \delta_{\boldsymbol{kq}}. \tag{20}$$

Thus, the sum in (18) takes the form

$$\sum_{ps}(\epsilon-\epsilon_s)g_{ni,ps}(\epsilon)g_{ps,mj}(\epsilon) = \sum_{ps}\sum_{\tau\nu}\sum_{\boldsymbol{k}}\frac{\langle i|\tau\boldsymbol{k}\rangle\langle\tau\boldsymbol{k}|s\rangle\langle s|\nu\boldsymbol{k}\rangle\langle\nu\boldsymbol{k}|j\rangle}{(\epsilon-\epsilon^{\tau}_{\boldsymbol{k}})(\epsilon-\epsilon^{\nu}_{\boldsymbol{k}})}(\epsilon-\epsilon_s)\exp[-\mathrm{i}\boldsymbol{k}\cdot(\boldsymbol{R}^n-\boldsymbol{R}^m)]. \quad (21)$$

To proceed with the remaining sums let us write the equations defining the projections $C^{\tau}_{\boldsymbol{k}s}\equiv\langle\tau\boldsymbol{k}|s\rangle$

$$\begin{aligned}(\epsilon-\epsilon_p)C^{\tau}_{\boldsymbol{k}ps} &= \sum_u t_{\boldsymbol{k}ps,du}C^{\tau}_{\boldsymbol{k}du}\\ (\epsilon-\epsilon_d)C^{\tau}_{\boldsymbol{k}ds} &= \sum_u t^{+}_{\boldsymbol{k}ps,du}C^{\tau}_{\boldsymbol{k}pu}.\end{aligned} \quad (22)$$

Here $C_{\boldsymbol{k}d}$ and $C_{\boldsymbol{k}p}$ are the amplitudes of the wavefunction on the metal-ion and oxygen ion, respectively; $\epsilon_p$ and $\epsilon_d$ are the energies of the p and d orbitals.

Let us multiply the first equation by $C^{\nu}_{\boldsymbol{k}ps}$, and the second equation by $C^{\tau}_{\boldsymbol{k}ds}$. Having found the difference between the results, one can obtain the relation

$$(\epsilon-\epsilon_p)\sum_s C^{\tau^*}_{\boldsymbol{k}ps}C^{\nu}_{\boldsymbol{k}ps} = (\epsilon-\epsilon_d)\sum_u C^{\tau^*}_{\boldsymbol{k}du}C^{\nu}_{\boldsymbol{k}du}. \quad (23)$$

We can add to this relation the orthogonality condition

$$\sum_s C^{\tau^*}_{\boldsymbol{k}ps}C^{\nu}_{\boldsymbol{k}ps}+\sum_u C^{\tau^*}_{\boldsymbol{k}du}C^{\nu}_{\boldsymbol{k}du} = \delta_{\tau\nu}. \quad (24)$$

It can be readily found from these equations that

$$\begin{aligned}\sum_s C^{\tau^*}_{\boldsymbol{k}ps}C^{\nu}_{\boldsymbol{k}ps} &= \frac{\epsilon-\epsilon_d}{2(\epsilon-\epsilon_0)}\delta_{\tau\nu}\\ \sum_u C^{\tau^*}_{\boldsymbol{k}du}C^{\nu}_{\boldsymbol{k}du} &= \frac{\epsilon-\epsilon_p}{2(\epsilon-\epsilon_0)}\delta_{\tau\nu}\end{aligned} \quad (25)$$

where $\epsilon_0$ is the half-sum of $\epsilon_p$ and $\epsilon_d$.

The expression obtained holds only for those bands in which $C_{\boldsymbol{k}d}\neq 0$. If this condition fails, then

$$\sum_s C^{\tau^*}_{\boldsymbol{k}ps}C^{\nu}_{\boldsymbol{k}ps} = \delta_{\tau\nu}. \quad (26)$$

The former case corresponds to the bonding and antibonding states while the latter corresponds to the non-bonding bands.

Inserting the result obtained into sum (15), we have

$$\sum_{ps}(\epsilon-\epsilon_s)g_{ni,ps}(\epsilon)g_{ps,mj}(\epsilon) = \frac{(\epsilon-\epsilon_d)(\epsilon-\epsilon_p)}{\epsilon-\epsilon_0}\sum_{\boldsymbol{k}\tau}{}'\frac{\langle i|\tau\boldsymbol{k}\rangle\langle\tau\boldsymbol{k}|j\rangle}{(\epsilon-\epsilon^{\tau}_{\boldsymbol{k}})^2}\exp[-\mathrm{i}\boldsymbol{k}\cdot(\boldsymbol{R}^n-\boldsymbol{R}^m)] + \frac{1}{\epsilon-\epsilon_p}\sum_{\tau}{}''\langle i|\tau\boldsymbol{k}\rangle\langle\tau\boldsymbol{k}|j\rangle\exp[-\mathrm{i}\boldsymbol{k}\cdot(\boldsymbol{R}^n-\boldsymbol{R}^m)]. \quad (27)$$

Here, the first sum is performed over the bonding and antibonding states and the second sum over the non-bonding bands. It is obvious that the second sum vanishes if $i$ or $j$ corresponds to a metal site.

One can express the remaining sums through the Green functions. Indeed

$$\sum_{k\tau}{}' \frac{\langle i|\tau k\rangle\langle \tau k|j\rangle}{(\epsilon-\epsilon_k^\tau)^2}\exp[-\mathrm{i}k\cdot(R^n-R^m)]$$
$$= -\frac{\mathrm{d}}{\mathrm{d}\epsilon}g_{ni,mj}(\epsilon)-\frac{1}{(\epsilon-\epsilon_p)^2}\sum_{\tau}{}''\sum_{k}\langle i|\tau k\rangle\langle\tau k|j\rangle\exp[-\mathrm{i}k\cdot(R^n-R^m)]. \quad (28)$$

The last sums in (27) and (28) do not vanish only in the cases when $ni = mj$ and the $i$th orbital lies on an oxygen ion. Both these conditions fail in our case. Thus, the final result is of the form

$$E_{cov}^{ni,mj} = f_{ni}V_{ni}\left[\frac{(\epsilon-\epsilon_d)(\epsilon-\epsilon_p)}{\epsilon-\epsilon_0}\frac{\mathrm{d}}{\mathrm{d}\epsilon}g_{ni,mj}(\epsilon)+g_{ni,mj}\right]f_{mj}V_{mj}. \quad (29)$$

It is seen that the energy of the indirect covalent interaction between the Ta sites is expressed through the non-diagonal element of the Green function and its derivative. By using expressions obtained for the Green functions in [6, 8] we have calculated these quantities and obtained $E_{cov}^{Ta,Ta} = -0.1$ eV. This implies that the energy of the indirect covalent interaction between the two Ta sites is much lower than the energy decrease caused by the lattice polarization. Thus, our computation shows that taking into account covalent bonding in $KTaO_3$ does not change the qualitative result previously obtained in [14]. The same can be said about the electric field asymptotic value outside the cluster used in [14]. Taking into account the correct asymptotic behaviour of the electric field also does not change the qualitative result obtained in [14]. Therefore, the main reason for the symmetry breaking at the oxygen vacancy in OPFs is the interaction between the electron captured by the vacancy and the lattice polarization. The decrease in the lattice polarization energy arose because the symmetry breaking is much greater than the covalent energy gain.

## 4. The electronic structure of $V_A$

In the cubic structure of OPFs of the $AMO_3$ kind, the A ion is surrounded by 12 equal oxygen ions. It was proposed in [24, 25] that a hole captured by a charged acceptor substituted in the A position can be localized on one of the 12 oxygen ions. The complex $A'_AO^-$ is evidently a dipole centre. The calculation of the polarization energy performed for this defect within a simple model of polarizable ions [14] showed that the polarization energy decreases when the hole is localized on a single oxygen ion instead of being spread over the 12 oxygen ions. The same result holds for the complex $V_AO^-$.

Figure 3 represents the results of our computation of the energies of the local states connected with the complex $V_{Sr}O^-$ in $SrTiO_3$. One can see that, when the perturbation potential $V_{ox}$ on the oxygen site is positive, the local levels are split off from the top of the valence band. This state is localized predominantly on the oxygen site. The evaluation of the perturbation potential by equation (5) gives the energy of the local ground state in the range from 0.1 to 0.2 eV.

The shell-model-based simulations of Lewis and Catlow [26] showed that holes are only weakly bound at barium vacancies in $BaTiO_3$. This result is in good agreement with our data. This point will be discussed more carefully in a separate part of our work devoted to experimental results.

## 5. Theory of optical excitations of $V_O^+$ in oxides of the perovskite family

By means of the absorption of a quantum, the electron located on one of two Ta ions nearest to the vacancy can be transferred to one of five nearest oxygen ions. The absorption coefficient is proportional to the probability of this process:

$$\gamma(\omega) = \frac{1}{\Omega}\int \mathrm{d}^3k \left| \sum_{i=1}^{5} \langle d\mathrm{Ta}|\hat{M}|p\mathrm{O}i\rangle C_{kpi} \right|^2 \delta(\epsilon_{\pi k} - \epsilon - h\omega) \tag{30}$$

where $C_{kpi}$ is the amplitude of the Bloch wave in a conduction band on the $i$th oxygen ion nearest the Ta ion, $\epsilon_{\pi k}$ is the energy dispersion in the $\pi$-conduction band, $\epsilon$ is the energy of the local state, $h\omega$ is the energy of the quantum and $\hat{M}$ is the operator of the interaction between an electron and light. Note that the direct transfer of an electron in the conduction band between two Ta sites is not realistic because of the very long distance between them (about 4 Å). However, the electron excitation from the Ta ion to the O ions is possible because of covalent bonding which causes mixing of the Ta and O states in the conduction bands.

By using the Wolfram–Ellialtioglu [17] model together with the theory of optical spectra developed in [9, 11, 27] we have performed the integration in (30) analytically. After averaging the result over the directions of the light polarization and summing over the $\pi$ bands the final expression becomes

$$\gamma(\omega) = \frac{1}{8h\omega(\xi + \Delta)}[(1 - \eta - 2\eta^2)K(\eta') + 2E(\eta')] \tag{31}$$

where

$$\begin{gathered}\eta = \kappa - \xi^2/4D^2 \qquad \eta' = \sqrt{1-\eta^2} \qquad \xi = \epsilon + h\omega - \epsilon_0 \qquad \kappa = \frac{\Delta^2 + 4D^2}{4} \\ K(\lambda) = \int_0^1 \frac{\mathrm{d}x}{\sqrt{(1-x^2)(1-\lambda^2x^2)}} \\ E(\lambda) = \int_0^1 \frac{\sqrt{(1-\lambda^2x^2)}\,\mathrm{d}x}{\sqrt{1-x^2}}.\end{gathered} \tag{32}$$

Here $K(\lambda)$ and $E(\lambda)$ are the complete elliptic integrals of the first and second kinds, respectively, $2\Delta$ is the width of the forbidden gap, $D$ is the (pd$\pi$) interaction integral and $\epsilon_0$ is the energy of the middle of the forbidden gap. Figure 4 shows the calculated shape of the spectrum for $SrTiO_3$.

In accordance with the experiment [28], the spectrum has a maximum at approximately 1.7 eV. The nature of this maximum is complex. It arises only because of the absence of an oxygen ion near the M site, i.e. because of the point symmetry breaking at the M site nearest to the vacancy. To check this assumption we have performed a model calculation of the optical spectrum of a substitution located at the M site and having the same energy level as $V_O^+$, but we have not found the band with the maximum at 1.7 eV. Thus, our calculation supports the idea [28] that the large energy of the optical excitation of $V_O^+$ is connected with the fact that the electron is mainly transferred to the states having large energy with respect to the bottom of the conduction band.

Thus, in our model, the dispersion in the optical spectra of $V_O^+$ is explained by the fact that the electron is excited to a conduction band having a large width (of approximately 3 eV). Contrary to this the optical spectrum of $Fe^{3+}$ impurities has very narrow bands. This can be accounted for because, in this case, the electron transition takes place between the $\pi$ and $\sigma$ levels (figure 2).

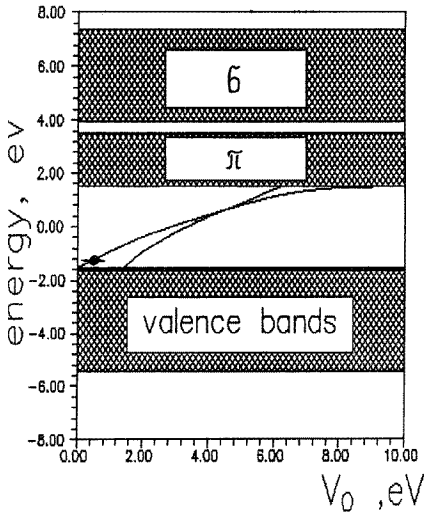


**Figure 3.** The dependence of the local state energies on the perturbation potential on an oxygen site nearest to the Sr position in $SrTiO_3$.

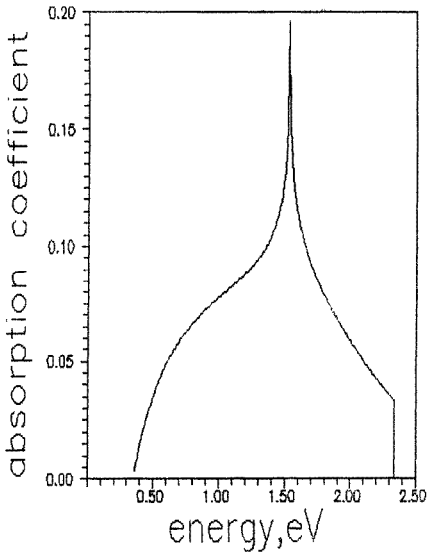


**Figure 4.** The calculated shape of the absorption spectrum of $V_O^+$ in $SrTiO_3$ (arbitrary units).

In our model we did not take into account the interaction between the electron and phonons. Nevertheless, the possibility of explaining the optical spectrum of $V_O^+$ by the polaron absorption (intervalence charge transfer) does exist. Apparently, both factors (the dispersion in the conduction band and the interaction between the electron and phonons) are important. Thus the theory needs to be developed in this respect.

## 6. The interaction between microscopic dipoles in polar crystals

In this section we shall discuss the interaction between microscopic dipoles and charges in polar lattices. By using the mode proposed in [29], we have found the asymptotic behaviour of the potential and electric field produced by a point charge and by a point dipole in the

simple-cubic lattice. The result is the following:

$$\varphi = \frac{1}{\epsilon R}\left[1 + 0.422\frac{(\epsilon-1)^2}{\epsilon}\left(\frac{a}{R}\right)^2 + \cdots\right] \tag{33}$$

$$E_z = \frac{\epsilon+2}{3\epsilon}\frac{1}{R^2}\left[1 + 2.11\frac{(\epsilon-1)(\epsilon-\frac{3}{5})}{\epsilon}\left(\frac{a}{R}\right)^2 + \cdots\right] \tag{34}$$

$$C_{zz} = \left(\frac{\epsilon+2}{3}\right)^2\frac{2}{\epsilon R^3}\left[1 + 5.908\frac{(\epsilon-1)(\epsilon-\frac{3}{7})}{\epsilon}\left(\frac{a}{R}\right)^2 + \cdots\right] \tag{35}$$

where $\varphi$ is the asymptotic of the potential produced by a point charge, $E_z$ is the electric field asymptotic, $C_{zz}$ is the asymptotic of the electric field produced by a point dipole, $R$ is the distance between unit cells and $a$ is the lattice parameter. Note that the usual relation between the potential and electric field does not hold because $R$ is not a continuous quantity here. There are additional terms in the potential in the case when the charge or point of view is shifted from the lattice site [29].

It is seen from equation (34) that the electric field produced by a point charge in the simple-cubic lattice is enhanced by the coefficient $\mu = (\epsilon + 2)/3$. The interaction between two dipoles is enhanced by $\mu^2$. These results were obtained in [30, 31].

The new result is the following. One can see from equation (24) that the distance where the asymptotic behaviour is valid has to satisfy the condition

$$R \gg a\sqrt{5.908\frac{(\epsilon-1)(\epsilon-\frac{3}{7})}{\epsilon}}. \tag{36}$$

At large $\epsilon$ we have

$$R \gg a(5.908\epsilon)^{1/2}. \tag{37}$$

The result obtained shows that the region where the crystal is polarized by a point defect is very large and increases with increasing $\epsilon$. Thus, one can expect that, as the oxygen vacancy is charged and has a dipole moment, it may strongly polarize surrounding media. In particular, this can cause an even-field current [32] or even phase transitions [33, 34].

Note that our statement does not contradict the fact that the potential produced by the oxygen vacancy vanishes at small distances. Indeed, it is seen from equation (33) that, at large $R$, the asymptotic of the potential is proportional to $1/\epsilon R$ whereas the asymptotic of the electric field does not depend on $\epsilon$ at large $\epsilon$. This implies that, at large distances, the potential on the lattice site is small but the electric field is not small. It should be remembered that we are discussing the local electric potential and local electric field on the lattice site. These quantities can differ from the averaged values greatly. It is obvious that the average electric field as well as the average electric potential are very small at large $\epsilon$. The reason for the electric field enhancement is the difference between the local and average electric fields.

## 7. Conclusions

In the present work a model of the electronic structure of intrinsic point defects is proposed. The oxygen vacancies $V_O$ and $V_O^+$ as well as the vacancy in the A position were considered. The computed data represented in the paper are consistent with the following statements.

The oxygen vacancy capturing an electron has an eigenstate with an energy of a few tenths of an electronvolt. This state is localized at an M ion nearest to the vacancy. As

this centre is charged, it also has a dipole moment with respect to the empty oxygen site. The dipole moment may be readily changed by applying an external electric or mechanical field. The energy of the maximum in the optical absorption spectrum of $V_O^+$ far exceeds the thermal activation energy. The neutral oxygen vacancy has to be ionized at room temperature owing to the small value of the first ionization potential.

The data obtained are consistent with experimental results on optical spectra [28] and electroconductivity [35]. A careful comparison between the theory and experiments will be carried out in part II of this paper.

## References


[1] Moretti P and Michel-Calendini F M 1986 *Solid State Commun.* **58** 613
[2] Michel-Calendini F M and Moretti P 1983 *Phys. Rev.* B **27** 763
[3] Michel-Calendini F M 1984 *Solid State Commun.* **52** 167
[4] Bunin M A, Prosandeyev S A, Gegusin I I and Tennenboum I M 1995 *Radiat. Eff. Defects Solids* **134** 75
[5] Selme M O and Pecheur P 1983 *J. Phys. C: Solid State Phys.* **16** 2559
[6] Prosandeyev S A, Fisenko A V and Sachenko V P 1984 *Ukr. Phys. J.* **29** 1338
[7] Fisenko A V, Prosandeyev S A and Sachenko V P 1986 *Phys. Status Solidi* b **137** 187
[8] Prosandeyev S A, Fisenko A V and Nebogatikov N M 1987 *Fiz. Tverd. tela* **29** 2600
[9] Prosandeyev S A, Fisenko A V, Vinnikov E V, Maksimov S M, Sachenko V P and Kupriyanova N M 1985 *Ukr. Phys. J.* **30** 465
[10] Prosandeyev S A, Fisenko A V, Sachenko V P and Kupriyanova N M 1987 *Ukr. Phys. J.* **32** 1690
[11] Prosandeyev S A 1990 *Electronic Structure and Physical Properties of Ion-Covalent Crystals* (Rostov On Don: Rostov State University) p 116 (in Russian)
[12] Prosandeyev S A, Teslenko N M and Fisenko A V 1993 *Izv. Akad. Nauk. SSSR* **57** 69
[13] Prosandeyev S A, Teslenko N M and Fisenko A V 1993 *J. Phys.: Condens. Matter* **5** 9327
[14] Prosandeyev S A and Osipenko I A 1995 *Phys. Status Solidi* b **192** 37
[15] Donnerberg H 1994 *Phys. Rev.* B **50** 9053
[16] Mattheiss L F 1972 *Phys. Rev.* B **6** 4718
[17] Wolfram T and Ellialtioglu S 1982 *Phys. Rev.* B **25** 2697
[18] Selme M O and Pecheur P 1988 *J. Phys. C: Solid State Phys.* **21** 1779
[19] Bernholc J and Pantelides S T 1978 *Phys. Rev.* B **18** 1780
[20] Abarenkov I V and Antonova I M 1974 *Phys. Status Solidi* b **65** 325
[21] Slater J C 1978 *The Self-Consistent Field for Molecules and Solids* (Moscow: Mir) p 61
[22] Fisher C, Auf der Horst C, Voigt P, Kapphan S and Zhao J 1995 *Radiat. Eff. Defects Solids* **136** 85
[23] Prosandeyev S A and Riabchinski A I 1996 *J. Phys.: Condens. Matter* **8** 505
[24] Wertz J E, Auzing P and Auzing J W 1959 *Disc. Faraday Soc.* **28** 136
[25] Shirmer O F, Berlinger W and Muller K A 1976 *Solid State Commun.* **18** 1505
[26] Lewis G V and Catlow C R A 1986 *J. Phys. Chem. Solids* **47** 89
[27] Prosandeyev S A and Tarasevich Yu Yu 1994 *Ferroelectrics* **164** 303
[28] Lee C, Destry J and Brebner J L 1975 *Phys. Rev.* B **11** 2299
[29] Mahan G D and Mazo R M 1968 *Phys. Rev.* **175** 1191
[30] Mahan G D 1967 *Phys. Rev.* **153** 983
[31] Vugmeister B E and Glinchuk M D 1990 *Rev. Mod. Phys.* **62** 993
[32] Prosandeyev S A, Chervonobrodov S P and Tennenboum I M 1994 *Ferroelectrics* **153** 279
[33] Prosandeyev S A and Tennenboum I M 1994 *J. Phys.: Condens. Matter* **6** 7013
[34] Gavriliachenko V G, Barabanova L A, Cixockii E S, Pavelchik M, Kupriyanov M F, Fesenko E G and Suroviak Z 1980 *Prace Fiz.* **8** 64
[35] Maksimov S M, Prokopalo O I, Raevski I P, Prosandeyev S A, Fisenko A V and Sachenko V P 1985 *Fiz. Tverd. tela* **27** 917